Filomat 36:1 (2022), 15–29
https://doi.org/10.2298/FIL2201015Y

Published by Faculty of Sciences and Mathematics,
University of Niš, Serbia
Available at: http://www.pmf.ni.ac.rs/filomat

Defect-Deferred Correction Method for the Non-Stationary Coupled Stokes/Darcy Model

Yanan Yang[a], Pengzhan Huang[a]

[a] *College of Mathematics and System Sciences, Xinjiang University, Urumqi 830046, P.R. China*

Abstract. This paper develops the defect-deferred correction method to solve the non-stationary coupled Stokes/Darcy model. This method is a combination of defect correction method and deferred correction method. And it can not only achieve the second order accuracy in time, but also be applied to the problem with small viscosity and hydraulic conductivity coefficients. The theoretical proof of the stability and the second order accuracy in time are shown. Some numerical experiments are given to verify the error convergence order in time. In addition, compared with the standard Galerkin finite element method, the advantages of the presented method in calculating small viscosity and hydraulic conductivity coefficients will also be reflected in the numerical experiments.

1. Introduction

In recent years, the coupling between incompressible flow and porous media flow has received more and more attention in many current industries, such as soil pollution problem, oil drilling simulation and filtering surface water and so on. Therefore, it is practical and necessary to develop some effective numerical methods to investigate the Stokes/Darcy model.

In fact, the Stokes/Darcy model has different governing equations in different regions and possesses multiple physical quantities. These characteristics have caused various difficulties and problems in the numerical simulation of the model. Nevertheless, many numerical calculation methods for solving Stokes/Darcy model have been proposed [1, 7, 11, 17–19, 25]. Qin and Hou have added time filter to the backward Euler scheme of the Stokes/Darcy model to improve the accuracy of the time from the first order to the second order. Also, They achieved that the addition of the time filter can increase the BDF2 scheme from the second order to the third order [21]. Further, Li, Zheng and Layton have analyzed a multi-rate decoupling algorithm that allows different time steps to be used in different sub-domains and improves the calculation accuracy and efficiency [26]. There are also the discontinuous Galerkin methods [23], interface relaxation methods [4] and decoupled methods based on two-grid or multi-grid finite element [5, 9, 16, 20] and so on.

The defect-deferred correction method was first proposed by Aggul, Connors, Erkmen, and Labovsky when solving the problem of fluid-fluid interaction [2]. For this method, it is a combination of defect

2020 *Mathematics Subject Classification*. Primary 65M12; Secondary 65M15
Keywords. Second order accuracy Small viscosity/hydraulic conductivity Defect-deferred correction method Stokes/Darcy model
Received: 14 December 2020; Revised: 09 March 2021; Accepted: 10 July 2021
Communicated by Marko Nedeljkov
Corresponding author: Pengzhan Huang
Research supported by the Natural Science Foundation of China (grant number 11861067) and Natural Science Foundation of Xinjiang Province (grant number 2021D01E11).
Email addresses: yangyn996@sina.com (Yanan Yang), hpzh007@yahoo.com (Pengzhan Huang)

correction method and deferred correction method. The defect correction method starts from a stable, low-order, and inexpensive method, and proceeds by calculating a series of approximate solutions on the same grid, gradually improving the accuracy. It uses a simple and effective artificial viscosity approximation to increase the viscosity coefficient of the flow. After that, a deferred correction method was established on this basis and applied to the data-passing scheme [8, 10] to create an unconditionally stable second-order precision partition time method. The combination of the defect correction and deferred correction was successfully tested in application to the one-domain Navier-Stokes equations [3] and the two-domain convection dominated convection diffusion problem [10].

In this paper, the defect-deferred correction method is mainly used to solve the numerical solutions of the Stokes/Darcy model with small viscosity and hydraulic conductivity coefficients. As the viscosity coefficient and hydraulic conductivity coefficient become smaller, the error of the standard Galerkin finite element method will increase rapidly. The defect-deferred correction method proposed not only achieves the second order accuracy in time, but also keeps the calculation results stable when the viscosity and hydraulic conductivity coefficients in the Stokes/Darcy model are small.

The rest of the paper is arranged as follows: The second section of this article mainly describes Stokes/Darcy model and preliminary work. The third section is devoted to the proof of stability and the error estimates of the fully discrete scheme. Finally, two numerical experiments verify the second order accuracy in time and the superiority of the algorithm for small viscosity/hydraulic conductivity coefficients in the Stokes/Darcy model.

2. Coupled Stokes/Darcy model

Let us take into account the model for coupling fluid and porous media flows in a bound smooth domain $\Omega \subset \mathbb{R}^2$, which consists of two sub-domains Ω_f and Ω_p simply. Interface Γ divides Ω into Ω_p and Ω_f, i.e. $\Omega = \Omega_p \cup \Omega_f$. Next, the boundary $\Gamma_f = \partial\Omega_f \cap \partial\Omega$, $\Gamma_p = \partial\Omega_p \cap \partial\Omega$ and interface $\Gamma = \partial\Omega_f \cap \partial\Omega_p$ are introduced. In the rest of this paper, we always use boldface characters to denote vectors or vector valued spaces. $\mathbf{n}_p$ and $\mathbf{n}_f$ represent the unit outward normal vectors of $\partial\Omega_p$ and $\partial\Omega_f$, respectively. The motion in fluid region Ω_f is governed by the Stokes equations [21, 22]:

$$\begin{aligned} &\frac{\partial \mathbf{u}_f}{\partial t} - \nabla \cdot (\mathbb{T}_v(\mathbf{u}_f, p_f)) = \mathbf{g}_f, && \text{in } \Omega_f, \\ &\nabla \cdot \mathbf{u}_f = 0, && \text{in } \Omega_f, \\ &\mathbf{u}_f(\mathbf{x}, 0) = \mathbf{u}_f^0(\mathbf{x}), && \text{in } \Omega_f, \end{aligned} \tag{1}$$

where $\mathbb{T}_v(\mathbf{u}_f, p_f) = -p_f\mathbb{I} + 2\nu\mathbb{D}(\mathbf{u}_f)$ is the stress tensor and $\mathbb{D}(\mathbf{u}_f) = \frac{1}{2}(\nabla\mathbf{u}_f + \nabla^{\mathrm{T}}\mathbf{u}_f)$ is the deformation rate tensor. $\mathbb{I}$ is the identity tensor and is expressed as

$$\mathbb{I} = \begin{bmatrix} 1 & 0 \\ 0 & 1 \end{bmatrix},$$

ν is the kinetic viscosity and $\mathbf{g}_f(\mathbf{x}, t)$ is the external force. The motion in porous medium region Ω_p is governed by

$$\begin{aligned} &\frac{S_0 \partial \phi_p}{\partial t} - \nabla \cdot \mathbb{K}\nabla\phi_p = g_p, && \text{in } \Omega_p, \\ &\phi_p(\mathbf{x}, 0) = \phi_p^0(\mathbf{x}), && \text{in } \Omega_p, \end{aligned} \tag{2}$$

where S_0 is the water storage coefficient. $\mathbb{K}$ represents the hydraulic conductivity in Ω_p, which is the positive symmetric tensor, and is allowed to change in space. The $g_p(\mathbf{x}, t)$ is a source term with a solvability condition $\int_{\Omega_p} g_p(\mathbf{x}, t) = 0$. The above equations (1) and (2) are coupled together by the following boundary conditions,

$$\mathbf{u}_f = 0, \ \text{ on } \Gamma_f, \quad \phi_p = 0, \ \text{ on } \Gamma_p, \tag{3}$$

and the interface conditions on Γ,

$$\begin{aligned}
&\mathbf{u}_f \cdot \mathbf{n}_f - \mathbb{K}\nabla\phi_p \cdot \mathbf{n}_p = 0,\\
&-[\mathbb{T}_v(\mathbf{u}_f, p_f)\cdot \mathbf{n}_f]\cdot \mathbf{n}_f = g\phi_p,\\
&-[\mathbb{T}_v(\mathbf{u}_f, p_f)\cdot \mathbf{n}_f]\cdot \tau = \frac{\sqrt{2}\alpha\nu}{\sqrt{\text{trace}\boldsymbol{\Pi}}}\mathbf{u}_f\cdot\tau,
\end{aligned} \tag{4}$$

where τ is the orthonormal tangential unit vectors along Γ. α is an experimentally validated parameter and $\boldsymbol{\Pi}$ represents the permeability. Here g represents the gravitational constant. The interface condition is called the Beavers-Joseph-Saffman interface condition [6, 13, 15, 24].

Then, let us introduce some function spaces:

$$\begin{aligned}
&\mathbf{X}_f = \{\mathbf{v}_f \in \mathbf{H^1}(\Omega_f) : \mathbf{v}_f|_{\Gamma_f} = 0\}, \quad X_p = \{\psi_p \in H^1(\Omega_p) : \psi_p|_{\Gamma_p} = 0\},\\
&Q_f = L^2(\Omega_f), \qquad\qquad \mathbf{U} = \mathbf{X}_f \times X_p.
\end{aligned}$$

We equip the domain D ($D = \Omega_p$ or Ω_f) with the usual L^2-scalar product $(\cdot,\cdot)_D$ and L^2-norm $\|\cdot\|_D$, which is expressed as $\|\cdot\|_{L^2}$. On the interface Γ, the L^2 inner product is defined as $(\cdot,\cdot)_\Gamma$. Besides, the space $\mathbf{X}_f$ and X_p are equipped with the following norms

$$\begin{aligned}
&\|\mathbf{v}_f\|_f = \|\nabla\mathbf{v}_f\|_{L^2} = \sqrt{(\nabla\mathbf{v}_f, \nabla\mathbf{v}_f)_{\Omega_f}}, \quad \forall \mathbf{v}_f \in \mathbf{X}_f,\\
&\|\psi_p\|_p = \|\nabla\psi_p\|_{L^2} = \sqrt{(\nabla\psi_p, \nabla\psi_p)_{\Omega_p}}, \quad \forall \psi_p \in X_p.
\end{aligned}$$

And the space $\mathbf{U}$ equipped with the norms: $\forall \underline{\mathbf{u}} = (\mathbf{u}_f, \phi_p)^{\mathrm{T}} \in \mathbf{U}$,

$$\begin{aligned}
&\|\underline{\mathbf{u}}\|_0 = \sqrt{(\mathbf{u}_f, \mathbf{u}_f)_{\Omega_f}} + \sqrt{gS_0(\phi_p, \phi_p)_{\Omega_p}},\\
&\|\underline{\mathbf{u}}\|_{\mathrm{U}} = \sqrt{\nu(\nabla\mathbf{u}_f, \nabla\mathbf{u}_f)_{\Omega_f}} + \sqrt{g\mathbb{K}(\nabla\phi_p, \nabla\phi_p)_{\Omega_p}}.
\end{aligned}$$

For functions $v(x,t)$, we define the norms,

$$\|v\|_{L^2(0,T;\mathbf{L^2}(\Omega))} = \left(\int_0^T \|v(\cdot,t)\|_{L^2}^2 \mathrm{d}t\right)^{\frac{1}{2}}, \quad \|v\|_{L^\infty(0,T;\mathbf{L^2}(\Omega))} = \operatorname*{ess\,sup}_{(0<t<T)} \|v(\cdot,t)\|_{L^2}.$$

Then the variational formulation for the time-dependent Stokes/Darcy model as follows: For $\mathbf{g}_f \in L^2(0,T;\mathbf{L^2}(\Omega_f))$ and $g_p \in L^2(0,T;L^2(\Omega_p))$, find $\underline{\mathbf{u}} = (\mathbf{u}_f, \phi_p)^{\mathrm{T}} \in L^2(0,T;\mathbf{X}_f) \cap L^\infty(0,T;\mathbf{L^2}(\Omega_f)) \times L^2(0,T;X_p) \cap L^\infty(0,T;L^2(\Omega_p))$ and $p_f \in L^2(0,T;Q_f)$ such that $\forall(\underline{\mathbf{v}}, q_f) \in \mathbf{U}\times Q_f$ satisfying

$$\begin{aligned}
&(\underline{\mathbf{u}}_t, \underline{\mathbf{v}}) + a(\underline{\mathbf{u}}, \underline{\mathbf{v}}) - b(\underline{\mathbf{v}}, p_f) + b(\underline{\mathbf{u}}, q_f) = \langle \mathbf{F}, \underline{\mathbf{v}}\rangle_{\mathbf{U}'},\\
&\underline{\mathbf{u}}(\mathbf{x}, 0) = \underline{\mathbf{u}}^0,
\end{aligned} \tag{5}$$

where

$$\begin{aligned}
&(\underline{\mathbf{u}}_t, \underline{\mathbf{v}}) = (\mathbf{u}_{f,t}, \mathbf{v}_f)_{\Omega_f} + (S_0\phi_{p,t}, \psi_p)_{\Omega_p}, \qquad a(\underline{\mathbf{u}}, \underline{\mathbf{v}}) = va_\Omega(\underline{\mathbf{u}}, \underline{\mathbf{v}}) + a_\Gamma(\underline{\mathbf{u}}, \underline{\mathbf{v}}),\\
&va_\Omega(\underline{\mathbf{u}}, \underline{\mathbf{v}}) = va_{\Omega_f}(\mathbf{u}_f, \mathbf{v}_f) + \mathbb{K}a_{\Omega_p}(\phi_p, \psi_p), \quad a_{\Omega_p}(\phi_p, \psi_p) = g(\nabla\phi_p, \nabla\psi_p)_{\Omega_p},\\
&a_{\Omega_f}(\mathbf{u}_f, \mathbf{v}_f) = (\nabla\mathbf{u}_f, \nabla\mathbf{v}_f)_{\Omega_f} + \left(\frac{\alpha\sqrt{d}}{\sqrt{\text{trace}\boldsymbol{\Pi}}}((\mathbf{u}_f, \mathbf{v}_f) - ((\mathbf{u}_f, \mathbf{v}_f)\cdot\mathbf{n}_f)\mathbf{n}_f)\right)_\Gamma,\\
&\langle \mathbf{F}, \underline{\mathbf{v}}\rangle_{\mathbf{U}'} = (\mathbf{g}_f, \mathbf{v}_f)_{\Omega_f} + g(g_p, \psi_p)_{\Omega_p}, \qquad a_\Gamma(\underline{\mathbf{u}}, \underline{\mathbf{v}}) = g(\phi_p, \mathbf{v}_f\cdot\mathbf{n}_f)_\Gamma - g(\psi_p, \mathbf{u}_f\cdot\mathbf{n}_f)_\Gamma,\\
&b(\underline{\mathbf{v}}, p_f) = (p_f, \nabla\cdot\mathbf{v}_f)_{\Omega_f},
\end{aligned}$$

where $\mathbf{U}'$ is the dual space of $\mathbf{U}$. The bilinear forms are continuous and coercive (refer to [7]). $\forall \underline{\mathbf{u}}, \underline{\mathbf{v}} \in \mathbf{U}$,

$$\begin{aligned}
&a(\underline{\mathbf{u}}, \underline{\mathbf{v}}) \le C_{con}\|\underline{\mathbf{u}}\|_{\mathrm{U}}\|\underline{\mathbf{v}}\|_{\mathrm{U}}, \quad a(\underline{\mathbf{u}}, \underline{\mathbf{u}}) \ge C_{coe}\|\underline{\mathbf{u}}\|_{\mathrm{U}}^2,\\
&a_\Gamma(\underline{\mathbf{u}}, \underline{\mathbf{v}}) \le C_\Gamma\|\underline{\mathbf{u}}\|_{\mathrm{U}}\|\underline{\mathbf{v}}\|_{\mathrm{U}}, \quad \forall \underline{\mathbf{u}}, \underline{\mathbf{v}} \in \mathbf{U},
\end{aligned} \tag{6}$$

where C_{con}, C_{coe} and C_Γ are positive constants and not dependent on the data of the problem. Additionally,

$$a_\Gamma(\underline{\mathbf{u}}, \underline{\mathbf{v}}) = -a_\Gamma(\underline{\mathbf{v}}, \underline{\mathbf{u}}) \quad \text{and} \quad a_\Gamma(\underline{\mathbf{u}}, \underline{\mathbf{u}}) = 0, \quad \forall \underline{\mathbf{u}}, \underline{\mathbf{v}} \in \mathbf{U}. \tag{7}$$

For the theoretical analysis, we introduce the trace and Poincaré inequalities. There exist positive constants C_p and $\tilde{C}_p$ that depend on the domain Ω_f and Ω_p respectively, such that for all $\mathbf{v}_f \in \mathbf{X}_f$ and $\psi_p \in X_p$,

$$\|\mathbf{v}_f\|_{L^2} \le C_p \|\mathbf{v}_f\|_f, \qquad \|\psi_p\|_{L^2} \le \tilde{C}_p \|\psi_p\|_p. \tag{8}$$

3. Two step defect-deferred correction

Firstly, let $\{t_n = n\Delta t\}_{n=0}^N$ be the mean of the time interval $[0, T]$, and the time step $\Delta t = \frac{T}{N}$. Secondly, τ_{fh} is constructed as regular triangles of Ω_f in 2D domain with max diameter h_f. Further, for Ω_p, we also define τ_{ph} with max diameter h_p. Then $h = \max\{h_f, h_p\}$ is set as the maximum diameter of Ω. For simplicity, we assume that Ω_f and Ω_p are smooth domains. Let $\mathbf{X}_{fh} \subset \mathbf{X}_f$, $Q_{fh} \subset Q_f$ and $X_{ph} \subset X_p$ are finite element spaces. Furthermore, the finite element space pair $(\mathbf{X}_{fh}, Q_{fh})$ is assumed to satisfy the usual discrete inf-sup condition or LBB condition for stability of the discrete pressure:

$$\inf_{q_{fh} \in Q_{fh}} \sup_{\mathbf{v}_h \in \mathbf{X}_{fh}} \frac{b(\mathbf{v}_h, q_{fh})}{\|\mathbf{v}_h\|_{\mathbf{X}_f} \|q_{fh}\|_{Q_f}} \ge \beta > 0,$$

where β is a constant and is independent of h. In fact, many finite element space pairs satisfy the discrete inf-sup condition, such as Taylor-Hood elements (P2-P1, P3-P2) and Scott-Vogelius element. In this paper, the theoretical analysis and numerical experiments are based on Taylor-Hood element (P2-P1). Then, we define $\mathbf{U}_h = (\mathbf{X}_{fh} \times X_{ph}) \subset (\mathbf{X}_f \times X_p)$. Throughout the remainder of this paper we will use $\mathbf{t}\underline{\mathbf{u}} = (\mathbf{t}\mathbf{u}_f, t\phi_p)$ and tp_f, $\underline{\hat{\mathbf{u}}}_h = (\hat{\mathbf{u}}_f, \hat{\phi}_p)$ and $\hat{p}_f$, $\mathbf{c}\underline{\mathbf{u}}_h = (\mathbf{c}\mathbf{u}_f, c\phi_p)$ and cp_f to denote the true solution, the defect step approximation and the defect-deferred correction step approximation respectively.

For $t \in [0, T]$, $\underline{\hat{\mathbf{u}}}_h^n$ and $\mathbf{c}\underline{\mathbf{u}}_h^n$ will denote the discrete approximation to $\mathbf{t}\underline{\mathbf{u}}^n$ $(n = 0, 1, \ldots, N)$. The artificial viscosity H is positive and chosen as a stabilization item. In order to facilitate the theoretical analysis below, we set $(\upsilon + H)a_\Omega(\underline{\mathbf{u}}, \underline{\mathbf{v}}) = (\nu + H)a_{\Omega_f}(\mathbf{u}_f, \mathbf{v}_f) + (\mathbb{K} + H\mathbb{I})a_{\Omega_p}(\phi_p, \psi_p)$. Discretely, divergence-free velocities will be sought in the test space

$$\mathbf{V}_h = \left\{ \mathbf{v}_h \in \mathbf{U}_h : \int_\Omega q_{fh} \nabla \cdot \mathbf{v}_h d\Omega = 0, \ \ \forall q_{fh} \in Q_{fh} \right\}.$$

In addition, there always exists the mesh-independent constant C and the finite elements $(\mathbf{u}_h, p_f) \in (\mathbf{U}_h, Q_{fh})$, that satisfy the following optimal approximation property [27]:

$$\|\mathbf{t}\underline{\mathbf{u}} - \mathbf{u}_h\|_0 \le Ch^3 \|\mathbf{t}\underline{\mathbf{u}}\|_{\mathbf{H}^3(\Omega)}, \quad \|\mathbf{t}\underline{\mathbf{u}} - \mathbf{u}_h\|_U \le Ch^2 \|\mathbf{t}\underline{\mathbf{u}}\|_{\mathbf{H}^2(\Omega)}. \tag{9}$$

After that, we will introduce the defect-deferred correction algorithm: Given $\underline{\hat{\mathbf{u}}}_h^n \in \mathbf{U}_h$, $\mathbf{c}\underline{\mathbf{u}}_h^n \in \mathbf{U}_h$, find $(\underline{\hat{\mathbf{u}}}_h^{n+1}, \hat{p}_f^{n+1}) \in (\mathbf{U}_h, Q_{fh})$, $(\mathbf{c}\underline{\mathbf{u}}_h^{n+1}, cp_f^{n+1}) \in (\mathbf{U}_h, Q_{fh})$ with $n = 0, 1, 2 \cdots N-1$, $\forall (\underline{\mathbf{v}}_h, q_{fh}) \in (\mathbf{U}_h, Q_{fh})$, satisfying

$$\left(\frac{\underline{\hat{\mathbf{u}}}_h^{n+1} - \underline{\hat{\mathbf{u}}}_h^n}{\Delta t}, \underline{\mathbf{v}}_h \right) + (\upsilon + H)a_\Omega(\underline{\hat{\mathbf{u}}}_h^{n+1}, \underline{\mathbf{v}}_h) + a_\Gamma(\underline{\hat{\mathbf{u}}}_h^{n+1}, \underline{\mathbf{v}}_h) - b(\underline{\mathbf{v}}_h, \hat{p}_f^{n+1}) = \langle \mathbf{F}^{n+1}, \underline{\mathbf{v}}_h \rangle_{\mathbf{U}'}, \tag{10}$$

and

$$\begin{aligned} &\left(\frac{\mathbf{c}\underline{\mathbf{u}}_h^{n+1} - \mathbf{c}\underline{\mathbf{u}}_h^n}{\Delta t}, \underline{\mathbf{v}}_h \right) + (\upsilon + H)a_\Omega(\mathbf{c}\underline{\mathbf{u}}_h^{n+1}, \underline{\mathbf{v}}_h) + a_\Gamma(\mathbf{c}\underline{\mathbf{u}}_h^{n+1}, \underline{\mathbf{v}}_h) - b(\underline{\mathbf{v}}_h, cp_f^{n+1}) = \\ &Ha_\Omega\left(\frac{\underline{\hat{\mathbf{u}}}_h^{n+1} + \underline{\hat{\mathbf{u}}}_h^n}{2}, \underline{\mathbf{v}}_h \right) + \left\langle \frac{\mathbf{F}^{n+1} + \mathbf{F}^n}{2}, \underline{\mathbf{v}}_h \right\rangle_{\mathbf{U}'} + (\upsilon + H)a_\Omega\left(\frac{\underline{\hat{\mathbf{u}}}_h^{n+1} - \underline{\hat{\mathbf{u}}}_h^n}{2}, \underline{\mathbf{v}}_h \right) \\ &+ a_\Gamma\left(\frac{\underline{\hat{\mathbf{u}}}_h^{n+1} - \underline{\hat{\mathbf{u}}}_h^n}{2}, \underline{\mathbf{v}}_h \right) - \frac{\Delta t}{2} b\left(\underline{\mathbf{v}}_h, \frac{\hat{p}_f^{n+1} - \hat{p}_f^n}{\Delta t} \right). \end{aligned} \tag{11}$$

(10) is the defect step and (11) is the defect-deferred correction step. The terms on the right hand side of (11) are written in a form that hints at the reason for the increased accuracy of the defect-deferred correction step solution. Note also that the matrix of the system is identical for (10) and (11) because of the similar structure on the left. Thus, a simple artificial viscosity data-passing approximation is computed twice to achieve higher accuracy while also having unconditional stability.

4. Stability and convergence

In this section, we prove the unconditional stability of both the defect step and the defect-deferred correction step approximations. Also the accuracy of defect step and defect-deferred correction step and time derivative step are shown.

Theorem 4.1. *(Stability of defect approximation) Let* $\underline{\hat{\mathbf{u}}}_h^{n+1}$ *with initial data* $\underline{\hat{\mathbf{u}}}_h^0$ *satisfy (10) for each* $n \in \{0, 1, 2, \cdots, N-1\}$. *Then we get*

$$\|\underline{\hat{\mathbf{u}}}_h^{n+1}\|_0^2 + \Delta t(\upsilon + H)C_{coe}\sum_{n=0}^{N-1}\|\underline{\hat{\mathbf{u}}}_h^{n+1}\|_U^2 \leq \frac{\Delta t(C_p^2 + \tilde{C}_p^2)}{C_{coe}(\upsilon + H)}\sum_{n=0}^{N-1}\|\mathbf{F}^{n+1}\|_{L^2}^2 + \|\underline{\hat{\mathbf{u}}}_h^0\|_0^2.$$

Proof. Taking $\underline{\mathbf{v}}_h = \underline{\hat{\mathbf{u}}}_h^{n+1} \in \mathbf{V}_h$ in (10), it follows that

$$\left(\frac{\underline{\hat{\mathbf{u}}}_h^{n+1} - \underline{\hat{\mathbf{u}}}_h^n}{\Delta t}, \underline{\hat{\mathbf{u}}}_h^{n+1}\right) + (\upsilon + H)a_\Omega(\underline{\hat{\mathbf{u}}}_h^{n+1}, \underline{\hat{\mathbf{u}}}_h^{n+1}) + a_\Gamma(\underline{\hat{\mathbf{u}}}_h^{n+1}, \underline{\hat{\mathbf{u}}}_h^{n+1}) = \langle \mathbf{F}^{n+1}, \underline{\hat{\mathbf{u}}}_h^{n+1}\rangle_{\mathbf{U}'}. \tag{12}$$

Using the Cauchy-Swcharz and Young's inequalities gives

$$\frac{\|\underline{\hat{\mathbf{u}}}_h^{n+1}\|_0^2 - \|\underline{\hat{\mathbf{u}}}_h^n\|_0^2}{2\Delta t} + (\upsilon + H)C_{coe}\|\underline{\hat{\mathbf{u}}}_h^{n+1}\|_{\mathrm{U}}^2 \leq \frac{C_{coe}(\upsilon + H)}{2}\|\underline{\hat{\mathbf{u}}}_h^{n+1}\|_{\mathrm{U}}^2 + \frac{(C_p^2 + \tilde{C}_p^2)}{2C_{coe}(\upsilon + H)}\|\mathbf{F}^{n+1}\|_{L^2}^2.$$

Multiplying by $2\Delta t$ and summing over the time levels, there holds

$$\|\underline{\hat{\mathbf{u}}}_h^{n+1}\|_0^2 + \Delta t(\upsilon + H)C_{coe}\sum_{n=0}^{N-1}\|\underline{\hat{\mathbf{u}}}_h^{n+1}\|_{\mathrm{U}}^2 \leq \frac{\Delta t(C_p^2 + \tilde{C}_p^2)}{C_{coe}(\upsilon + H)}\sum_{n=0}^{N-1}\|\mathbf{F}^{n+1}\|_{L^2}^2 + \|\underline{\hat{\mathbf{u}}}_h^0\|_0^2. \tag{13}$$

□

Theorem 4.2. *(Stability of defect-deferred correction approximation) Let* $\mathbf{c}\underline{\mathbf{u}}_h^{n+1}$ *with initial data* $\mathbf{c}\underline{\mathbf{u}}_h^0$ *satisfy (11) for each* $n \in \{0, 1, 2, \cdots, N-1\}$. *Then* $\exists C > 0$ *is independent of* h *and* Δt *such that* $\mathbf{c}\underline{\mathbf{u}}_h^{n+1}$ *satisfies*

$$\|\mathbf{c}\underline{\mathbf{u}}_h^{n+1}\|_0^2 + (\upsilon + H)\Delta t\sum_{n=0}^{N-1}C_{coe}\|\mathbf{c}\underline{\mathbf{u}}_h^{n+1}\|_U^2 \leq C\left\{\|\mathbf{c}\underline{\mathbf{u}}_h^0\|_0^2 + \Delta t\sum_{n=0}^{N-1}\|\frac{\mathbf{F}^{n+1} + \mathbf{F}^n}{2}\|_{L^2}^2 + \|\underline{\hat{\mathbf{u}}}_h^0\|_0^2\right\}.$$

Proof. Taking $\underline{\mathbf{v}}_h = \mathbf{c}\underline{\mathbf{u}}_h^{n+1} \in \mathbf{V}_h$ in (11) obtains

$$\begin{aligned}&\left(\frac{\mathbf{c}\underline{\mathbf{u}}_h^{n+1} - \mathbf{c}\underline{\mathbf{u}}_h^n}{\Delta t}, \mathbf{c}\underline{\mathbf{u}}_h^{n+1}\right) + (\upsilon + H)a_\Omega(\mathbf{c}\underline{\mathbf{u}}_h^{n+1}, \mathbf{c}\underline{\mathbf{u}}_h^{n+1}) + a_\Gamma(\mathbf{c}\underline{\mathbf{u}}_h^{n+1}, \mathbf{c}\underline{\mathbf{u}}_h^{n+1}) = \left\langle\frac{\mathbf{F}^{n+1} + \mathbf{F}^n}{2}, \mathbf{c}\underline{\mathbf{u}}_h^{n+1}\right\rangle_{\mathbf{U}'}\\ &+ Ha_\Omega\left(\frac{\underline{\hat{\mathbf{u}}}_h^{n+1} + \underline{\hat{\mathbf{u}}}_h^n}{2}, \mathbf{c}\underline{\mathbf{u}}_h^{n+1}\right) + (\upsilon + H)a_\Omega\left(\frac{\underline{\hat{\mathbf{u}}}_h^{n+1} - \underline{\hat{\mathbf{u}}}_h^n}{2}, \mathbf{c}\underline{\mathbf{u}}_h^{n+1}\right) + a_\Gamma\left(\frac{\underline{\hat{\mathbf{u}}}_h^{n+1} - \underline{\hat{\mathbf{u}}}_h^n}{2}, \mathbf{c}\underline{\mathbf{u}}_h^{n+1}\right).\end{aligned} \tag{14}$$

Using the Cauchy-Swcharz and Young's inequalities, the right-hand sides of (14) are bounded as follows

$$\left\langle\frac{\mathbf{F}^{n+1} + \mathbf{F}^n}{2}, \mathbf{c}\underline{\mathbf{u}}_h^{n+1}\right\rangle_{\mathbf{U}'} \leq \epsilon C_{coe}(\upsilon + H)\|\mathbf{c}\underline{\mathbf{u}}_h^{n+1}\|_{\mathrm{U}}^2 + \frac{(C_p^2 + \tilde{C}_p^2)}{4\epsilon C_{coe}(\upsilon + H)}\|\frac{\mathbf{F}^{n+1} + \mathbf{F}^n}{2}\|_{L^2}^2,$$

$$Ha_\Omega\left(\frac{\hat{\underline{\mathbf{u}}}_h^{n+1}+\hat{\underline{\mathbf{u}}}_h^{n}}{2},\mathbf{c}\underline{\mathbf{u}}_h^{n+1}\right)\le 2\epsilon(\upsilon+H)C_{coe}\|\mathbf{c}\underline{\mathbf{u}}_h^{n+1}\|_{\mathrm{U}}^2+\frac{H^2C_{con}^2}{16\epsilon C_{coe}(\upsilon+H)}(\|\hat{\underline{\mathbf{u}}}_h^{n+1}\|_{\mathrm{U}}^2+\|\hat{\underline{\mathbf{u}}}_h^{n}\|_{\mathrm{U}}^2),$$

and

$$(\upsilon+H)a_\Omega\left(\frac{\hat{\underline{\mathbf{u}}}_h^{n+1}-\hat{\underline{\mathbf{u}}}_h^{n}}{2},\mathbf{c}\underline{\mathbf{u}}_h^{n+1}\right)\le 2\epsilon(\upsilon+H)C_{coe}\|\mathbf{c}\underline{\mathbf{u}}_h^{n+1}\|_{\mathrm{U}}^2+\frac{(\upsilon+H)C_{con}^2}{16\epsilon C_{coe}}(\|\hat{\underline{\mathbf{u}}}_h^{n+1}\|_{\mathrm{U}}^2+\|\hat{\underline{\mathbf{u}}}_h^{n}\|_{\mathrm{U}}^2),$$

$$a_\Gamma\left(\frac{\hat{\underline{\mathbf{u}}}_h^{n+1}-\hat{\underline{\mathbf{u}}}_h^{n}}{2},\mathbf{c}\underline{\mathbf{u}}_h^{n+1}\right)\le 2\epsilon(\upsilon+H)C_{coe}\|\mathbf{c}\underline{\mathbf{u}}_h^{n+1}\|_{\mathrm{U}}^2+\frac{C_\Gamma^2}{16\epsilon(\upsilon+H)C_{coe}}(\|\hat{\underline{\mathbf{u}}}_h^{n+1}\|_{\mathrm{U}}^2+\|\hat{\underline{\mathbf{u}}}_h^{n}\|_{\mathrm{U}}^2).$$

Choosing $\epsilon=\frac{1}{14}$ and multiplying by $2\Delta t$, we obtain

$$\begin{aligned}&\|\mathbf{c}\underline{\mathbf{u}}_h^{n+1}\|_0^2-\|\mathbf{c}\underline{\mathbf{u}}_h^{n}\|_0^2+\Delta t(\upsilon+H)C_{coe}\|\mathbf{c}\underline{\mathbf{u}}_h^{n+1}\|_{\mathrm{U}}^2\le\frac{7(C_p^2+\tilde{C}_p^2)\Delta t}{C_{coe}(\upsilon+H)}\|\frac{\mathbf{F}^{n+1}+\mathbf{F}^n}{2}\|_{L^2}^2\\&+\frac{7H^2C_{con}^2\Delta t}{4(\upsilon+H)C_{coe}}(\|\hat{\underline{\mathbf{u}}}_h^{n+1}\|_{\mathrm{U}}^2+\|\hat{\underline{\mathbf{u}}}_h^{n}\|_{\mathrm{U}}^2)+\frac{7C_\Gamma^2\Delta t}{4(\upsilon+H)C_{coe}}(\|\hat{\underline{\mathbf{u}}}_h^{n+1}\|_{\mathrm{U}}^2+\|\hat{\underline{\mathbf{u}}}_h^{n}\|_{\mathrm{U}}^2)\\&+\frac{7(\upsilon+H)C_{con}^2\Delta t}{4C_{coe}}(\|\hat{\underline{\mathbf{u}}}_h^{n+1}\|_{\mathrm{U}}^2+\|\hat{\underline{\mathbf{u}}}_h^{n}\|_{\mathrm{U}}^2).\end{aligned}\tag{15}$$

□

Next, we start by proving the accuracy estimate of the defect solution.

Theorem 4.3. *(Accuracy of defect step) Let* $\mathbf{t}\underline{\mathbf{u}}$ *be smooth enough and* $\phi_h^0=0$. *Then* $\exists C>0$ *is independent of* h *and* Δt *such that for any* $n\in\{0,1,2,\cdots,N-1\}$, *the solution* $\hat{\underline{\mathbf{u}}}_h^{n+1}$ *of* (11) *satisfies*

$$\|\mathbf{t}\underline{\mathbf{u}}^{n+1}-\hat{\underline{\mathbf{u}}}_h^{n+1}\|_0^2+\Delta t(\upsilon+H)C_{coe}\sum_{n=0}^{N-1}\|\mathbf{t}\underline{\mathbf{u}}^{n+1}-\hat{\underline{\mathbf{u}}}_h^{n+1}\|_U^2\le C(h^4+\Delta t^2+H^2).$$

Proof. Write (5) at time t_{n+1} as

$$\begin{aligned}&\left(\frac{\mathbf{t}\underline{\mathbf{u}}^{n+1}-\mathbf{t}\underline{\mathbf{u}}^{n}}{\Delta t},\underline{\mathbf{v}}_h\right)+(\upsilon+H)a_\Omega(\mathbf{t}\underline{\mathbf{u}}^{n+1},\underline{\mathbf{v}}_h)+a_\Gamma(\mathbf{t}\underline{\mathbf{u}}^{n+1},\underline{\mathbf{v}}_h)-b(\underline{\mathbf{v}}_h,tp_f^{n+1})\\&=\langle\mathbf{F}^{n+1},\underline{\mathbf{v}}_h\rangle_{\mathrm{U}'}+\left(\frac{\mathbf{t}\underline{\mathbf{u}}^{n+1}-\mathbf{t}\underline{\mathbf{u}}^{n}}{\Delta t}-\mathbf{t}\underline{\mathbf{u}}_t^{n+1},\underline{\mathbf{v}}_h\right)+Ha_\Omega(\mathbf{t}\underline{\mathbf{u}}^{n+1},\underline{\mathbf{v}}_h).\end{aligned}\tag{16}$$

The errors are decomposed as $\mathbf{e}_h^{n+1}=(\bar{\mathbf{u}}_h^{n+1}-\hat{\underline{\mathbf{u}}}_h^{n+1})-(\bar{\mathbf{u}}_h^{n+1}-\mathbf{t}\underline{\mathbf{u}}^{n+1})=\phi_h^{n+1}-\eta_h^{n+1}$. Denote $\rho^{n+1}=\frac{\mathbf{t}\underline{\mathbf{u}}^{n+1}-\mathbf{t}\underline{\mathbf{u}}^{n}}{\Delta t}-\mathbf{t}\underline{\mathbf{u}}_t^{n+1}$, subtract (10) from (16) to obtain the equation for the error.

$$\begin{aligned}&\left(\frac{\mathbf{e}_h^{n+1}-\mathbf{e}_h^{n}}{\Delta t},\underline{\mathbf{v}}_h\right)+(\upsilon+H)a_\Omega(\mathbf{e}_h^{n+1},\underline{\mathbf{v}}_h)+a_\Gamma(\mathbf{e}_h^{n+1},\underline{\mathbf{v}}_h)-b(\underline{\mathbf{v}}_h,tp_f^{n+1}-\hat{p}_f^{n+1})=(\rho^{n+1},\underline{\mathbf{v}}_h)\\&+Ha_\Omega(\mathbf{t}\underline{\mathbf{u}}^{n+1},\underline{\mathbf{v}}_h).\end{aligned}\tag{17}$$

Taking $\underline{\mathbf{v}}_h=\phi_h^{n+1}\in\mathbf{V}_h$, we have

$$\begin{aligned}&\left(\frac{\phi_h^{n+1}-\phi_h^{n}}{\Delta t},\phi_h^{n+1}\right)+(\upsilon+H)a_\Omega(\phi_h^{n+1},\phi_h^{n+1})+a_\Gamma(\phi_h^{n+1},\phi_h^{n+1})=(\rho^{n+1},\phi_h^{n+1})\\&+Ha_\Omega(\mathbf{t}\underline{\mathbf{u}}^{n+1},\phi_h^{n+1})+\left(\frac{\eta_h^{n+1}-\eta_h^{n}}{\Delta t},\phi_h^{n+1}\right)+a_\Gamma(\eta_h^{n+1},\phi_h^{n+1})+(\upsilon+H)a_\Omega(\eta_h^{n+1},\phi_h^{n+1}).\end{aligned}\tag{18}$$

On the one hand, the left-hand sides of (18) are shown as follows:

$$\begin{aligned}&\frac{\|\phi_h^{n+1}\|_0^2-\|\phi_h^n\|_0^2}{2\Delta t}+(\upsilon+H)C_{coe}\|\phi_h^{n+1}\|_{\mathrm{U}}^2\le(\rho^{n+1},\phi_h^{n+1})+Ha_\Omega(\underline{\mathbf{tu}}^{n+1},\phi_h^{n+1})\\&+\left(\frac{\eta_h^{n+1}-\eta_h^n}{\Delta t},\phi_h^{n+1}\right)+a_\Gamma(\eta_h^{n+1},\phi_h^{n+1})+(\upsilon+H)a_\Omega(\eta_h^{n+1},\phi_h^{n+1}).\end{aligned}\tag{19}$$

On the other hand, we find a bound on the right term with the Cauchy-Swcharz inequalities and Young inequalities,

$$(\rho^{n+1},\phi_h^{n+1})\le\epsilon(\upsilon+H)C_{coe}\|\phi_h^{n+1}\|_{\mathrm{U}}^2+\frac{(C_p^2+\tilde{C}_p^2)}{4\epsilon(\upsilon+H)C_{coe}}\|\rho^{n+1}\|_0^2,$$

$$Ha_\Omega(\underline{\mathbf{tu}}^{n+1},\phi_h^{n+1})\le\epsilon(\upsilon+H)C_{coe}\|\phi_h^{n+1}\|_{\mathrm{U}}^2+\frac{H^2C_{con}^2}{4\epsilon(\upsilon+H)C_{coe}}\|\underline{\mathbf{tu}}^{n+1}\|_{\mathrm{U}}^2,$$

$$\left(\frac{\eta_h^{n+1}-\eta_h^n}{\Delta t},\phi_h^{n+1}\right)\le\epsilon(\upsilon+H)C_{coe}\|\phi_h^{n+1}\|_{\mathrm{U}}^2+\frac{(C_p^2+\tilde{C}_p^2)}{4\epsilon(\upsilon+H)C_{coe}}\|\frac{\eta_h^{n+1}-\eta_h^n}{\Delta t}\|_0^2.$$

Similarly,

$$a_\Gamma(\eta_h^{n+1},\phi_h^{n+1})\le\epsilon(\upsilon+H)C_{coe}\|\phi_h^{n+1}\|_{\mathrm{U}}^2+\frac{C_\Gamma^2}{4\epsilon(\upsilon+H)C_{coe}}\|\eta_h^{n+1}\|_{\mathrm{U}}^2,$$

$$(\upsilon+H)a_\Omega(\eta_h^{n+1},\phi_h^{n+1})\le\epsilon(\upsilon+H)C_{coe}\|\phi_h^{n+1}\|_{\mathrm{U}}^2+\frac{(\upsilon+H)C_{con}^2}{4\epsilon C_{coe}}\|\eta_h^{n+1}\|_{U}^2.$$

Choosing $\epsilon=\frac{1}{10}$ and multiplying by $2\Delta t$, we have

$$\begin{aligned}&\|\phi_h^{n+1}\|_0^2-\|\phi_h^n\|_0^2+\Delta t(\upsilon+H)C_{coe}\|\phi_h^{n+1}\|_{\mathrm{U}}^2\le\frac{5\Delta t(C_p^2+\tilde{C}_p^2)}{(\upsilon+H)C_{coe}}\|\rho^{n+1}\|_0^2\\&+\frac{5\Delta tH^2C_{con}^2}{(\upsilon+H)C_{coe}}\|\underline{\mathbf{tu}}^{n+1}\|_{\mathrm{U}}^2+\frac{5\Delta t(C_p^2+\tilde{C}_p^2)}{(\upsilon+H)C_{coe}}\|\frac{\eta_h^{n+1}-\eta_h^n}{\Delta t}\|_0^2\\&+\frac{5\Delta t(\upsilon+H)C_{con}^2}{C_{coe}}\|\eta_h^{n+1}\|_{\mathrm{U}}^2+\frac{5\Delta tC_\Gamma^2}{(\upsilon+H)C_{coe}}\|\eta_h^{n+1}\|_{\mathrm{U}}^2+\frac{5\Delta t(\upsilon+H)C_{con}^2}{C_{coe}}\|\eta_h^{n+1}\|_{U}^2.\end{aligned}\tag{20}$$

Summing over the time levels allow us to obtain

$$\begin{aligned}&\|\phi_h^{n+1}\|_0^2+\Delta t(\upsilon+H)C_{coe}\sum_{n=0}^{N-1}\|\phi_h^{n+1}\|_{\mathrm{U}}^2\le\frac{5\Delta t^2(C_p^2+\tilde{C}_p^2)}{(\upsilon+H)C_{coe}}\|\underline{\mathbf{tu}}_{tt}\|_{L^2(0,T;\mathbf{U})}^2\\&+\frac{5\Delta tH^2C_{con}^2}{(\upsilon+H)C_{coe}}\sum_{n=0}^{N-1}\|\underline{\mathbf{tu}}^{n+1}\|_{\mathrm{U}}^2+\frac{5\Delta t(C_p^2+\tilde{C}_p^2)}{(\upsilon+H)C_{coe}}\sum_{n=0}^{N-1}\|\frac{\eta_h^{n+1}-\eta_h^n}{\Delta t}\|_0^2\\&+\frac{5\Delta t(\upsilon+H)C_{con}^2}{C_{coe}}\sum_{n=0}^{N-1}\|\eta_h^{n+1}\|_{\mathrm{U}}^2+\frac{5\Delta tC_\Gamma^2}{(\upsilon+H)C_{coe}}\sum_{n=0}^{N-1}\|\eta_h^{n+1}\|_{\mathrm{U}}^2+\frac{5\Delta t(\upsilon+H)C_{con}^2}{C_{coe}}\sum_{n=0}^{N-1}\|\eta_h^{n+1}\|_{U}^2.\end{aligned}$$

Finally, combine $\frac{1}{\upsilon+H}<\frac{1}{\upsilon}$ and the triangle inequality to obtain

$$\|\underline{\mathbf{tu}}^{n+1}-\underline{\hat{\mathbf{u}}}_h^{n+1}\|_0^2+\Delta t(\upsilon+H)C_{coe}\sum_{n=0}^{N-1}\|\underline{\mathbf{tu}}^{n+1}-\underline{\hat{\mathbf{u}}}_h^{n+1}\|_{\mathrm{U}}^2\le C(h^4+\Delta t^2+H^2).$$

□

Before providing the accuracy estimate for the defect-deferred correction approximation, we need to give

Theorem 4.4. *(Accuracy of time derivative of the error in the defect step) Let the assumption of Theorem* 4.3 *holds. Then* $\exists C \geq 0$ *is independent of* h *and* Δt *such that for any* $n \in \{0, 1, 2 \cdot \cdot, N-1\}$. *The discrete time derivative of the error* $\frac{\mathbf{e}_h^{n+1}-\mathbf{e}_h^n}{\Delta t}$ *satisfies*

$$\|\frac{\mathbf{e}_h^{n+1}-\mathbf{e}_h^n}{\Delta t}\|_0^2 + \Delta t(\upsilon + H)C_{coe}\sum_{n=0}^{N-1}\|\frac{\mathbf{e}_h^{n+1}-\mathbf{e}_h^n}{\Delta t}\|_U^2 \leq C(h^4 + \Delta t^2 + H^2).$$

Proof. Taking $\underline{\mathbf{v}}_h = \frac{\phi_h^{n+1}-\phi_h^n}{\Delta t} \in \mathbf{V}_h$ in (17) leads to

$$\begin{aligned}&\left(\frac{\mathbf{e}_h^{n+1}-\mathbf{e}_h^n}{\Delta t}, \frac{\phi_h^{n+1}-\phi_h^n}{\Delta t}\right) + (\upsilon + H)a_\Omega\left(\mathbf{e}_h^{n+1}, \frac{\phi_h^{n+1}-\phi_h^n}{\Delta t}\right) + a_\Gamma\left(e_h^{n+1}, \frac{\phi_h^{n+1}-\phi_h^n}{\Delta t}\right)\\ &= \left(\rho^{n+1}, \frac{\phi_h^{n+1}-\phi_h^n}{\Delta t}\right) + Ha_\Omega\left(\underline{\mathbf{tu}}^{n+1}, \frac{\phi_h^{n+1}-\phi_h^n}{\Delta t}\right).\end{aligned} \tag{21}$$

Also, take $\underline{\mathbf{v}}_h = \frac{\phi_h^{n+1}-\phi_h^n}{\Delta t}$ in (17) at the previous time level, and subtract the resulting equation from (21). Denoting $S_h^{n+1} \equiv \frac{\phi_h^{n+1}-\phi_h^n}{\Delta t}$ to get

$$\begin{aligned}&(S_h^{n+1} - S_h^n, S_h^{n+1}) + \Delta t(\upsilon + H)a_\Omega(S_h^{n+1}, S_h^{n+1}) + \Delta t a_\Gamma(S_h^{n+1}, S_h^{n+1})\\ &\leq \Delta t\left(\frac{\eta_h^{n+1} - 2\eta_h^n + \eta_h^{n-1}}{\Delta t^2}, S_h^{n+1}\right) + \Delta t\left(\frac{\rho^{n+1}-\rho^n}{\Delta t}, S_h^{n+1}\right) + \Delta t a_\Gamma\left(\frac{\eta_h^{n+1}-\eta_h^n}{\Delta t}, S_h^{n+1}\right)\\ &+ \Delta t H a_\Gamma\left(\frac{\underline{\mathbf{tu}}^{n+1}-\underline{\mathbf{tu}}^n}{\Delta t}, S_h^{n+1}\right) + \Delta t(\upsilon + H)a_\Omega\left(\frac{\eta^{n+1}-\eta^n}{\Delta t}, S_h^{n+1}\right).\end{aligned} \tag{22}$$

Followed by the Cauchy-Swcharz and Young's inequalities, and combine the conclusion of (9) to obain

$$\begin{aligned}&\Delta t\left(\frac{\eta_h^{n+1} - 2\eta_h^n + \eta_h^{n-1}}{\Delta t^2}, S_h^{n+1}\right) \leq \Delta t\epsilon(\upsilon + H)C_{coe}\|S_h^{n+1}\|_{\mathrm{U}}^2 + \frac{(C_p^2 + \tilde{C}_p^2)}{4\epsilon(\upsilon + H)C_{coe}}\|\eta_{h,tt}^{n+1}\|_0^2,\\ &\Delta t\left(\frac{\rho^{n+1}-\rho^n}{\Delta t}, S_h^{n+1}\right) \leq \Delta t\epsilon(\upsilon + H)C_{coe}\|S_h^{n+1}\|_{\mathrm{U}}^2 + \frac{\Delta t(C_p^2 + \tilde{C}_p^2)}{4\epsilon(\upsilon + H)C_{coe}}\|\frac{\rho^{n+1}-\rho^n}{\Delta t}\|_0^2.\end{aligned}$$

Similarly,

$$\begin{aligned}&\Delta t a_\Gamma\left(\frac{\eta_h^{n+1}-\eta_h^n}{\Delta t}, S_h^{n+1}\right) \leq \Delta t\epsilon(\upsilon + H)C_{coe}\|S_h^{n+1}\|_{\mathrm{U}}^2 + \frac{C_\Gamma^2}{4\epsilon(\upsilon + H)C_{coe}}\|\eta_{h,t}^{n+1}\|_{\mathrm{U}}^2,\\ &\Delta t H a_\Gamma\left(\frac{t\underline{\mathbf{u}}^{n+1}-\underline{\mathbf{tu}}^n}{\Delta t}, S_h^{n+1}\right) \leq \Delta t\epsilon(\upsilon + H)C_{coe}\|S_h^{n+1}\|_{\mathrm{U}}^2 + \frac{\Delta t H^2 C_{con}^2}{4\epsilon(\upsilon + H)C_{coe}}\|\frac{\underline{\mathbf{tu}}^{n+1}-\underline{\mathbf{tu}}^n}{\Delta t}\|_{\mathrm{U}}^2,\\ &\Delta t(\upsilon + H)a_\Omega\left(\frac{\eta^{n+1}-\eta^n}{\Delta t}, S_h^{n+1}\right) \leq \Delta t\epsilon(\upsilon + H)C_{coe}\|S_h^{n+1}\|_{\mathrm{U}}^2 + \frac{(\upsilon + H)C_{con}^2}{4\epsilon C_{coe}}\|\eta_{h,t}^{n+1}\|_{\mathrm{U}}^2.\end{aligned}$$

Choosing $\epsilon = \frac{1}{10}$ leads to

$$\begin{aligned}&\|S_h^{n+1}\|_0^2 - \|S_h^n\|_0^2 + \Delta t(\upsilon + H)C_{coe}\|S_h^{n+1}\|_{\mathrm{U}}^2\\ &\leq \frac{5(C_p^2 + \tilde{C}_p^2)}{(\upsilon + H)C_{coe}}\|\eta_{h,tt}^{n+1}\|_0^2 + \frac{5\Delta t(C_p^2 + \tilde{C}_p^2)}{(\upsilon + H)C_{coe}}\|\frac{\rho^{n+1}-\rho^n}{\Delta t}\|_0^2 + \frac{5C_\Gamma^2}{(\upsilon + H)C_{coe}}\|\eta_{h,t}^{n+1}\|_{\mathrm{U}}^2\\ &+ \frac{5H^2C_{con}^2}{(\upsilon + H)C_{coe}}\|\underline{\mathbf{tu}}_t^{n+1}\|_{L^2(t_n,t_{n+1};\mathbf{U})}^2 + \frac{5(\upsilon + H)C_{con}^2}{C_{coe}}\|\eta_{h,t}^{n+1}\|_{\mathrm{U}}^2.\end{aligned}$$

Summing over the time levels obtain

$$\begin{aligned}\|S_h^{n+1}\|_0^2 + \Delta t(\upsilon + H)C_{coe}\sum_{n=0}^{N-1}\|S_h^{n+1}\|_{\mathrm{U}}^2 \le \frac{5(C_p^2+\tilde{C}_p^2)}{(\upsilon+H)C_{coe}}\sum_{n=0}^{N-1}\|\eta_{h,tt}^{n+1}\|_0^2 + \frac{5\Delta t^2(C_p^2+\tilde{C}_p^2)}{(\upsilon+H)C_{coe}}\|\underline{\mathbf{tu}}_{tt}\|^2_{L^\infty(0,T,\mathbf{L^2}(\Omega))}\\ + \frac{5C_\Gamma^2}{(\upsilon+H)C_{coe}}\sum_{n=0}^{N-1}\|\eta_{h,t}^{n+1}\|_{\mathrm{U}}^2 + \frac{5H^2C_{con}^2}{(\upsilon+H)C_{coe}}\|\underline{\mathbf{tu}}_t\|^2_{L^2(0,T,\mathbf{U})} + \frac{5(\upsilon+H)C_{con}^2}{C_{coe}}\sum_{n=0}^{N-1}\|\eta_{h,t}^{n+1}\|_{\mathrm{U}}^2 + \|S_h^1\|_0^2.\end{aligned} \tag{23}$$

In order to get a bound on $\|S_h^1\|_0^2$, consider (22) at $n = 0$. We choose $\underline{\hat{\mathbf{u}}}_h^0$ so that $(\underline{\mathbf{tu}}^0 - \underline{\hat{\mathbf{u}}}_h^0, \underline{\mathbf{v}}_h) = 0$. Thus, $\mathbf{e}^0 = -\eta^0$, $S_h^0 = 0$ and $\phi_h^0 = 0$. We take $\underline{\mathbf{v}}_h = S_h^1 = \frac{\phi_h^1 - \phi_h^0}{\Delta t} = \frac{\phi_h^1}{\Delta t} \in \mathbf{V}_h$ to obtain

$$\begin{aligned}&\|S_h^1\|_0^2 + \Delta t(\upsilon+H)a_\Omega(S_h^1,S_h^1) + \Delta t a_\Gamma(S_h^1,S_h^1)\\ &\quad\le (\rho^1,S_h^1) + Ha_\Gamma(\underline{\mathbf{tu}}^1,S_h^1) + \left(\frac{\eta_h^1-\eta_h^0}{\Delta t},S_h^1\right) + (\upsilon+H)a_\Omega(\eta_h^1,S_h^1) + a_\Gamma(\eta_h^1,S_h^1).\end{aligned} \tag{24}$$

The application of the Cauchy-Schwarz and Young inequalities gives the bounds

$$\begin{aligned}\|S_h^1\|_0^2 + \Delta t(\upsilon+H)C_{coe}\|S_h^1\|_{\mathrm{U}}^2 \le C\Big[\|\frac{\eta_h^1-\eta_h^0}{\Delta t}\|_0^2 + H^2\|\underline{\mathbf{tu}}^1\|^2_{L^2(t_0,t_1,\mathbf{U})}\\ + \Delta t^2\|\underline{\mathbf{tu}}_{tt}^1\|^2_{L^\infty(t_0,t_1,\mathbf{U})} + (\upsilon+H)\|\eta_h^1\|_{\mathrm{U}}^2 + \|\eta_h^1\|_{\mathrm{U}}^2 + \|S_h^0\|_0^2\Big].\end{aligned} \tag{25}$$

Combine (23), triangle inequality and $\frac{1}{\upsilon+H} < \frac{1}{\upsilon}$ to complete the proof

$$\|\frac{\mathbf{e}_h^{n+1}-\mathbf{e}_h^n}{\Delta t}\|_0^2 + \Delta t(\upsilon+H)C_{coe}\sum_{n=0}^{N-1}\|\frac{\mathbf{e}_h^{n+1}-\mathbf{e}_h^n}{\Delta t}\|_{\mathrm{U}}^2 \le C(h^4+\Delta t^2+H^2). \tag{26}$$

□

We finally give the proof of accuracy of the defect-deferred correction step solution.

Theorem 4.5. *(Accuracy of defect-deferred correction step) Let the assumption of Theorem* 4.3 *and Theorem* 4.4 *hold and* $\mathbf{c}\phi_h^0 = 0$*. Then* $C \ge 0$ *is independent of* h *and* Δt *such that for any* $n \in \{0,1,2\cdots,N-1\}$*, the solution* $\mathbf{c}\underline{\mathbf{u}}_h^{n+1}$ *of* (11) *satisfies*

$$\|\underline{\mathbf{tu}}^{n+1} - \mathbf{c}\underline{\mathbf{u}}_h^{n+1}\|_0^2 + \Delta t(\upsilon+H)C_{coe}\sum_{n=0}^{N-1}\|\underline{\mathbf{tu}}^{n+1} - \mathbf{c}\underline{\mathbf{u}}_h^{n+1}\|_U^2 \le C\Big[\Delta t^4 + h^4 + H^4 + h^2H^2 + \Delta t^2H^2 + \Delta t^2h^2\Big]. \tag{27}$$

Proof. Summing (5) at time levels t_n and t_{n+1} and dividing by 2, we obtain

$$\begin{aligned}&\left(\frac{\underline{\mathbf{tu}}^{n+1}-\underline{\mathbf{tu}}^n}{\Delta t},\underline{\mathbf{v}}_h\right) + (\upsilon+H)a_\Omega(\underline{\mathbf{tu}}^{n+1},\underline{\mathbf{v}}_h) + a_\Gamma(\underline{\mathbf{tu}}^{n+1},\underline{\mathbf{v}}_h) - b(\underline{\mathbf{v}}_h,tp_f^{n+1})\\ &= \left\langle\frac{\mathbf{F}^{n+1}+\mathbf{F}^n}{2},\underline{\mathbf{v}}_h\right\rangle_{\mathrm{U}'} + \left(\frac{\underline{\mathbf{tu}}^{n+1}-\underline{\mathbf{tu}}^n}{\Delta t} - \frac{\underline{\mathbf{tu}}_t^{n+1}+t\underline{\mathbf{u}}_t^n}{2},\underline{\mathbf{v}}_h\right) + Ha_\Omega\left(\frac{t\underline{\mathbf{u}}^{n+1}+\underline{\mathbf{tu}}^n}{2},\underline{\mathbf{v}}_h\right)\\ &\quad + (\upsilon+H)a_\Omega\left(\frac{\underline{\mathbf{tu}}^{n+1}-\underline{\mathbf{tu}}^n}{2},\underline{\mathbf{v}}_h\right) + a_\Gamma\left(\frac{\underline{\mathbf{tu}}^{n+1}-\underline{\mathbf{tu}}^n}{2},\underline{\mathbf{v}}_h\right) - \frac{\Delta t}{2}b\left(\underline{\mathbf{v}}_h,\frac{tp_f^{n+1}-tp_f^n}{\Delta t}\right).\end{aligned} \tag{28}$$

Denote $\gamma^{n+1} = \frac{\mathbf{t}\underline{\mathbf{u}}^{n+1}-\mathbf{t}\underline{\mathbf{u}}^{n}}{\Delta t} - \frac{\mathbf{t}\underline{\mathbf{u}}_t^{n+1}+\mathbf{t}\underline{\mathbf{u}}_t^{n}}{2}$, subtract (11) from (28) to obtain the equation for the error. Decompose the error $\mathbf{c}\mathbf{e}_h^{n+1} = (\ddot{\mathbf{u}}_h^{n+1} - \mathbf{c}\underline{\mathbf{u}}_h^{n+1}) - (\ddot{\mathbf{u}}_h^{n+1} - \mathbf{t}\underline{\mathbf{u}}^{n+1}) = \mathbf{c}\phi_h^{n+1} - \mathbf{c}\eta_h^{n+1}$. For $\underline{\mathbf{v}}_h = \mathbf{c}\phi_h^{n+1} \in \mathbf{V}_h$, we have

$$\begin{aligned}
&\left(\frac{\mathbf{c}\phi_h^{n+1}-\mathbf{c}\phi_h^{n}}{\Delta t}, \mathbf{c}\phi_h^{n+1}\right) + (\upsilon+H)a_\Omega(\mathbf{c}\phi_h^{n+1}, \mathbf{c}\phi_h^{n+1}) + a_\Gamma(\mathbf{c}\phi_h^{n+1}, \mathbf{c}\phi_h^{n+1}) = a_\Gamma(\mathbf{c}\eta_h^{n+1}, \mathbf{c}\phi_h^{n+1}) \\
&+ (\gamma^{n+1}, \mathbf{c}\phi_h^{n+1}) + Ha_\Omega\left(\frac{\mathbf{e}_h^{n+1}+\mathbf{e}_h^{n}}{2}, \mathbf{c}\phi_h^{n+1}\right) + \frac{\Delta t}{2}(\upsilon+H)a_\Omega\left(\frac{\mathbf{e}_h^{n+1}-\mathbf{e}_h^{n}}{\Delta t}, \mathbf{c}\phi_h^{n+1}\right) \\
&+ \frac{\Delta t}{2}a_\Gamma\left(\frac{\mathbf{e}_h^{n+1}-\mathbf{e}_h^{n}}{\Delta t}, \mathbf{c}\phi_h^{n+1}\right) + \left(\frac{\mathbf{c}\eta_h^{n+1}-\mathbf{c}\eta_h^{n}}{\Delta t}, \mathbf{c}\phi_h^{n+1}\right) + (\upsilon+H)a_\Omega(\mathbf{c}\eta_h^{n+1}, \mathbf{c}\phi_h^{n+1}).
\end{aligned} \tag{29}$$

Using the Cauchy-Swcharz and Young's inequalities, the right-hand sides of (29) are bounded as follows

$$\begin{aligned}
&a_\Gamma(\mathbf{c}\eta_h^{n+1}, \mathbf{c}\phi_h^{n+1}) \le \epsilon(\upsilon+H)C_{coe}\|\mathbf{c}\phi_h^{n+1}\|_{\mathrm{U}}^2 + \frac{C_\Gamma^2}{4\epsilon(\upsilon+H)C_{coe}}\|\mathbf{c}\eta_h^{n+1}\|_{\mathrm{U}}^2, \\
&(\gamma^{n+1}, \mathbf{c}\phi_h^{n+1}) \le \epsilon(\upsilon+H)C_{coe}\|\mathbf{c}\phi_h^{n+1}\|_{\mathrm{U}}^2 + \frac{(C_p^2+\tilde{C}_p^2)}{4\epsilon(\upsilon+H)C_{coe}}\|\gamma^{n+1}\|_0^2, \\
&Ha_\Omega\left(\frac{\mathbf{e}_h^{n+1}+\mathbf{e}_h^{n}}{2}, \mathbf{c}\phi_h^{n+1}\right) \le 2\epsilon(\upsilon+H)C_{coe}\|\mathbf{c}\phi_h^{n+1}\|_{\mathrm{U}}^2 + \frac{C_{con}^2H^2}{16\epsilon(\upsilon+H)C_{coe}}\|\mathbf{e}_h^{n+1}\|_{\mathrm{U}}^2 + \frac{C_{con}^2H^2}{16\epsilon(\upsilon+H)C_{coe}}\|\mathbf{e}_h^{n}\|_{\mathrm{U}}^2,
\end{aligned}$$

and

$$\begin{aligned}
&\frac{\Delta t}{2}(\upsilon+H)a_\Omega\left(\frac{\mathbf{e}_h^{n+1}-\mathbf{e}_h^{n}}{\Delta t}, \mathbf{c}\phi_h^{n+1}\right) \le \epsilon(\upsilon+H)C_{coe}\|\mathbf{c}\phi_h^{n+1}\|_{\mathrm{U}}^2 + \frac{\Delta t^2(\upsilon+H)C_{con}^2}{16\epsilon C_{coe}}\|\frac{\mathbf{e}_h^{n+1}-\mathbf{e}_h^{n}}{\Delta t}\|_{\mathrm{U}}^2, \\
&\frac{\Delta t}{2}a_\Gamma\left(\frac{\mathbf{e}_h^{n+1}-\mathbf{e}_h^{n}}{\Delta t}, \mathbf{c}\phi_h^{n+1}\right) \le \epsilon(\upsilon+H)C_{coe}\|\mathbf{c}\phi_h^{n+1}\|_{\mathrm{U}}^2 + \frac{C_\Gamma^2\Delta t^2}{16\epsilon(\upsilon+H)C_{coe}}\|\frac{\mathbf{e}_h^{n+1}-\mathbf{e}_h^{n}}{\Delta t}\|_{\mathrm{U}}^2, \\
&(\upsilon+H)a_\Omega(\mathbf{c}\eta_h^{n+1}, \mathbf{c}\phi_h^{n+1}) \le \epsilon(\upsilon+H)C_{coe}\|\mathbf{c}\phi_h^{n+1}\|_{\mathrm{U}}^2 + \frac{C_\Gamma^2(\upsilon+H)}{4\epsilon C_{coe}}\|\mathbf{c}\eta_h^{n+1}\|_{\mathrm{U}}^2.
\end{aligned}$$

Similarly,

$$\left(\frac{\mathbf{c}\eta_h^{n+1}-\mathbf{c}\eta_h^{n}}{\Delta t}, \mathbf{c}\phi_h^{n+1}\right) \le \epsilon(\upsilon+H)C_{coe}\|\mathbf{c}\phi_h^{n+1}\|_{\mathrm{U}}^2 + \frac{(C_p^2+\tilde{C}_p^2)}{4\epsilon(\upsilon+H)C_{coe}}\|\frac{\mathbf{c}\eta_h^{n+1}-\mathbf{c}\eta_h^{n}}{\Delta t}\|_0^2.$$

Choosing $\epsilon = \frac{1}{16}$ and multiplying by $2\Delta t$, we have

$$\begin{aligned}
&\|\mathbf{c}\phi_h^{n+1}\|_0^2 + (\upsilon+H)\Delta tC_{coe}\|\mathbf{c}\phi_h^{n+1}\|_{\mathrm{U}}^2 - \|\mathbf{c}\phi_h^{n}\|_0^2 \le \frac{2C_{con}^2H^2\Delta t}{(\upsilon+H)C_{coe}}(\|\mathbf{e}_h^{n+1}\|_{\mathrm{U}}^2 + \|\mathbf{e}_h^{n}\|_{\mathrm{U}}^2) \\
&+ \frac{8(C_p^2+\tilde{C}_p^2)\Delta t}{(\upsilon+H)C_{coe}}\|\gamma^{n+1}\|_0^2 + \frac{2\Delta t^3C_{con}^2(\upsilon+H)}{C_{coe}}\|\frac{\mathbf{e}_h^{n+1}-\mathbf{e}_h^{n}}{\Delta t}\|_{\mathrm{U}}^2 + \frac{2\Delta t^3C_\Gamma^2}{C_{coe}(\upsilon+H)}\|\frac{\mathbf{e}_h^{n+1}-\mathbf{e}_h^{n}}{\Delta t}\|_{\mathrm{U}}^2 \\
&+ \frac{8(C_p^2+\tilde{C}_p^2)}{(\upsilon+H)C_{coe}}\|\mathbf{c}\eta_{h,t}^{n+1}\|_0^2 + \frac{8C_\Gamma^2\Delta t}{(\upsilon+H)C_{coe}}\|\mathbf{c}\eta_h^{n+1}\|_{\mathrm{U}}^2 + \frac{8C_\Gamma^2(\upsilon+H)\Delta t}{C_{coe}}\|\mathbf{c}\eta_h^{n+1}\|_{\mathrm{U}}^2.
\end{aligned} \tag{30}$$

Take $\frac{1}{\upsilon+H} < \frac{1}{\upsilon}$ and sum over the time levels to obtain

$$\begin{aligned}
\|\mathbf{c}\phi_h^{n+1}\|_0^2 + \Delta t(\upsilon+H)C_{coe}\sum_{n=0}^{N-1}\|\mathbf{c}\phi_h^{n+1}\|_{\mathrm{U}}^2 &\le \frac{8(C_p^2+\tilde{C}_p^2)\Delta t^4}{(\upsilon+H)C_{coe}}\|\underline{\mathbf{tu}}_{ttt}\|^2_{L^\infty(0,T,\mathbf{L^2}(\Omega))} \\
&+ \frac{2C_{con}^2H^2\Delta t}{(\upsilon+H)C_{coe}}\sum_{n=0}^{N-1}(\|\mathbf{e}_h^{n+1}\|_{\mathrm{U}}^2+\|\mathbf{e}_h^{n}\|_{\mathrm{U}}^2) + \frac{2\Delta t^3C_{con}^2(\upsilon+H)}{C_{coe}}\sum_{n=0}^{N-1}\|\frac{\mathbf{e}_h^{n+1}-\mathbf{e}_h^{n}}{\Delta t}\|_{\mathrm{U}}^2 \\
&+ \frac{2\Delta t^3C_\Gamma^2}{C_{coe}(\upsilon+H)}\sum_{n=0}^{N-1}\|\frac{\mathbf{e}_h^{n+1}-\mathbf{e}_h^{n}}{\Delta t}\|_{\mathrm{U}}^2 + \frac{8(C_p^2+\tilde{C}_p^2)}{(\upsilon+H)C_{coe}}\sum_{n=0}^{N-1}\|\mathbf{c}\eta_{h,t}^{n+1}\|_0^2 + \frac{8C_\Gamma^2\Delta t}{(\upsilon+H)C_{coe}}\sum_{n=0}^{N-1}\|\mathbf{c}\eta_h^{n+1}\|_{\mathrm{U}}^2 \\
&+ \frac{8C_\Gamma^2(\upsilon+H)\Delta t}{C_{coe}}\sum_{n=0}^{N-1}\|\mathbf{c}\eta_h^{n+1}\|_{\mathrm{U}}^2.
\end{aligned} \tag{31}$$

Then, combine the conclusions of Theorem 4.3, Theorem 4.4 and triangle inequality to complete the proof. □

5. Numerical experiments

In this section, some numerical tests are presented to verify the theoretical results obtained in the previous sections for the defect-deferred correction method. We use the well-known Taylor-Hood elements (P2-P1) for the fluid equation and the piecewise quadratic polynomials (P2) for the porous equation. Furthermore, we implemented the code using the software package FreeFEM++ [12].

5.1. Computational testing

All the physical parameters ρ, g, ν, α, S are simply set to 1, and $\mathbb{K}$ is simply set to $\mathbb{I}$. The final time is chosen as $T = 1$. The initial conditions, boundary conditions and the source terms follow from the exact solutions. We assume the area as $\Omega_f = [0,1]\times[1,2]$, $\Omega_p = [0,1]\times[0,1]$, $\Gamma = (0,1)\times\{1\}$ and give the exact solution:

$$\begin{aligned}
\mathbf{u}_f &= \Big((x^2(y-1)^2+y)\cos(t), -\frac{2}{3}x(y-1)^3\cos(t) + (2-\pi\sin(\pi x))\cos(t)\Big), \\
p_f &= (2-\pi\sin(\pi x))\sin(0.5\pi y)\cos(t), \\
\phi_p &= (2-\pi\sin(\pi x))(1-y-\cos(\pi y))\cos(t).
\end{aligned}$$

To confirm the accuracy, we set $h = \Delta t = H = \frac{1}{4}, \frac{1}{8}, \frac{1}{16}, \frac{1}{32}, \frac{1}{64}$ and calculate the errors and convergence rates for the variables $\mathbf{u}_f$, p_f and ϕ_p. Table 1 and Table 2 show the error and the convergence rates of the defect step $\hat{\mathbf{u}}_f$ and defect-deferred correction step $\mathbf{cu}_f$, respectively. Table 3 and Table 4 provide the error and convergence rates of the defect step ϕ_p and the defect-deferred correction step $c\phi_p$.

Table 1: Errors for defect step $\hat{\mathbf{u}}_f$ approximations

$1/\Delta t$	$\|\mathbf{u}_f-\hat{\mathbf{u}}_f\|_{L^2}$	Rate	$\|\mathbf{u}_f-\hat{\mathbf{u}}_f\|_{\mathrm{U}}$	Rate
4	1.48E−2	—	1.84E−1	—
8	8.16E−3	0.86	8.49E−2	1.12
16	4.40E−3	0.89	4.31E−2	0.98
32	2.29E−3	0.94	2.21E−2	0.96
64	1.17E−3	0.97	1.13E−2	0.97

Table 2: Errors for defect-deferred correction step $\mathbf{cu}_f$ approximations

$1/\Delta t$	$\|\mathbf{u}_f - \mathbf{cu}_f\|_{L^2}$	Rate	$\|\mathbf{u}_f - \mathbf{cu}_f\|_{\mathrm{U}}$	Rate
4	7.02E−3	—	1.37E−1	—
8	1.91E−3	1.88	3.77E−2	1.86
16	5.71E−4	1.74	1.02E−2	1.89
32	1.64E−4	1.80	2.69E−3	1.91
64	4.50E−5	1.86	7.05E−4	1.93

Table 3: Errors for defect step ϕ_p approximations

$1/\Delta t$	$\|\phi_p - \hat{\phi}_p\|_{L^2}$	Rate	$\|\phi_p - \hat{\phi}_p\|_{\mathrm{U}}$	Rate
4	1.81E−1	—	6.92E−1	—
8	1.03E−1	0.81	3.76E−1	0.88
16	5.53E−2	0.89	2.00E−1	0.91
32	2.88E−2	0.94	1.04E−1	0.95
64	1.47E−2	0.97	5.30E−2	0.97

Table 4: Errors for defect-deferred correction step $c\phi_p$ approximations

$1/\Delta t$	$\|\phi_p - c\phi_p\|_{L^2}$	Rate	$\|\phi_p - c\phi_p\|_{\mathrm{U}}$	Rate
4	5.90E−2	—	3.26E−1	—
8	1.79E−2	1.72	9.39E−2	1.79
16	5.08E−3	1.82	2.55E−2	1.88
32	1.37E−3	1.89	6.72E−3	1.92
64	3.62E−4	1.92	1.74E−3	1.94

From the four tables above, we can see that the error of defect-deferred correction steps is smaller than that of defect steps. In addition, the rates of the defect steps of Stokes velocity $\mathbf{u}_f$ and Darcy hydraulic head ϕ_p are all close to the first order. And the rates of the defect-deferred correction steps are all close to the second order. The numerical simulation calculation results are consistent with the theoretical analysis results.

5.2. Small parameters problem

In order to illustrate the advantage of the defect-deferred correction method in calculating small viscosity/hydraulic coefficients, we compare the discrete errors of the standard Galerkin finite element method and the defect-deferred correction method with the example mentioned in [14]. Specifically we consider the model problem on $\Gamma = (0, \pi) \times \{0\}$, where $\Omega_f = [0, \pi] \times [0, 1]$ and $\Omega_p = [0, \pi] \times [-1, 0]$. We take $\alpha = 1$, $g = 1$, $S_0 = 1$, varying ν, and

$$\mathbb{K} = \begin{bmatrix} K_{11} & 0 \\ 0 & K_{22} \end{bmatrix}.$$

The boundary condition functions and the source terms are chosen to follow the exact solutions,

$$\begin{aligned} \mathbf{u}_f &= \left(\frac{K_{11}}{\pi}\sin(2\pi y)\cos(x)e^t, (-2K_{22} + \frac{K_{22}}{\pi^2}\sin^2(\pi y))\sin(x)e^t\right), \\ p &= 0, \\ \phi &= (e^y - e^{-y})\sin(x)e^t. \end{aligned}$$

All the numerical results below are for the final time $T = 1$. We consider four groups of simulated numerical calculations (Figure 1–4) on K_{11} and K_{22} taking 10^{-2}, 10^{-3}, 10^{-4} and 10^{-5} separately. The results of each set of numerical simulations are shown in two graphs, which are the respective absolute errors of velocity and hydraulic head changes of the standard Galerkin finite element method and the defect-deferred correction method when the ν is 10^{-2}, 10^{-3}, 10^{-4} and 10^{-5}. The errors shown below are all calculated when $h = \Delta t = 1/32$. The stabilization item H in Figure 1 is 1/32, and in Figure 2–4 is 1/270. Before the numerical tests, $e^k_{\mathbf{u},h}$ and $e^k_{\phi,h}$ represent the discrete errors of velocity and hydraulic head, respectively. The results are as follows:

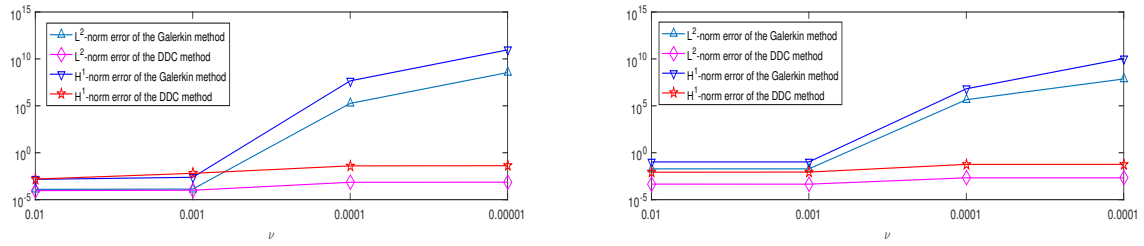

(a) (b)

Figure 1: $e^k_{\mathbf{u},h}$(a) and $e^k_{\phi,h}$(b) when $K_{11} = K_{22} = 10^{-2}$.

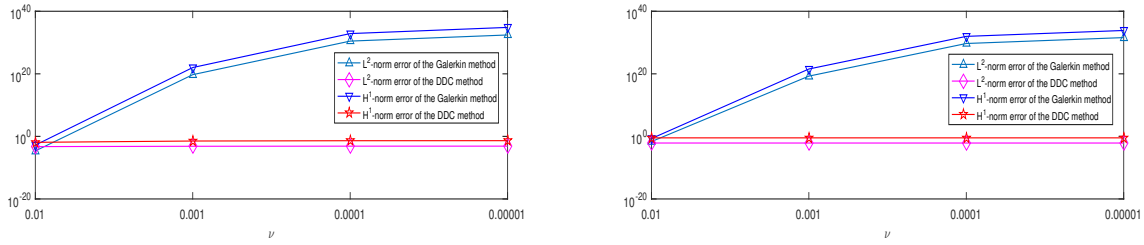

(a) (b)

Figure 2: $e^k_{\mathbf{u},h}$(a) and $e^k_{\phi,h}$(b) when $K_{11} = K_{22} = 10^{-3}$.

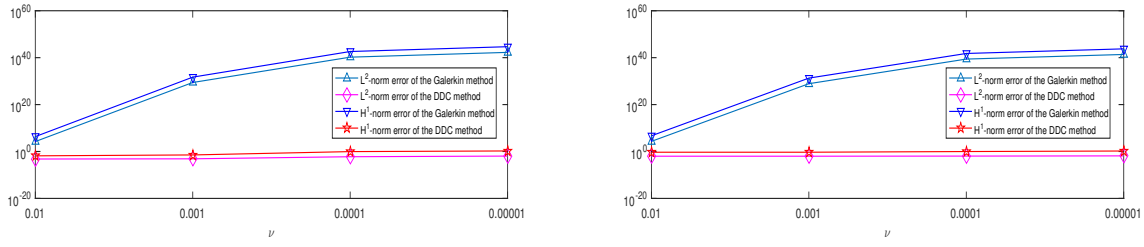

(a) (b)

Figure 3: $e^k_{\mathbf{u},h}$(a) and $e^k_{\phi,h}$(b) when $K_{11} = K_{22} = 10^{-4}$.

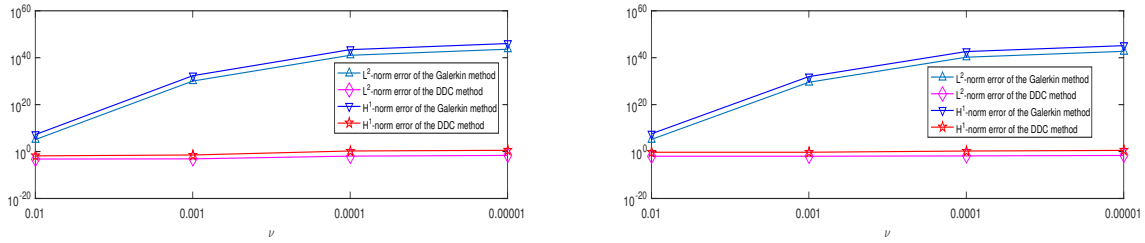

(a) (b)

Figure 4: $e^k_{\mathbf{u},h}$(a) and $e^k_{\phi,h}$(b) when $K_{11} = K_{22} = 10^{-5}$.

From the above four sets of results, we can see that when $K_{11} = K_{22} = 10^{-2}$ and $\nu = 10^{-3}$ /10^{-4}, the L^2-norm error and H^1-norm error of velocity and hydraulic head in the defect-deferred correction method has a slight advantage over the standard Galerkin finite element method. However, as ν becomes smaller, the calculation results of the standard Galerkin finite element method became divergent. But the calculation results of the defect-deferred correction method are convergent. This situation is more obvious in the other three sets of experiments where $K_{11} = K_{22} = 10^{-3}/10^{-4}/10^{-5}$.

References

[1] H. Abboud, V. Girault, T. Sayah, A second order accuracy for a full discretized time-dependent Navier-Stokes equations by a two-grid scheme, Numer. Math. 114 (2009) 189-231.
[2] M. Aggul, J. M. Connors, D. Erkmen, A. E. Labovsky, A defect-deferred correction method for fluid-fluid interaction, SIAM J. Numer. Anal. 56 (2018) 2484-2512.
[3] M. Aggul, A. Labovsky, A high accuracy minimally invasive regularization technique for Navier-Stokes equations at high reynolds number, Numer. Meth. Part. Differ. Equ. 33 (2016) 814-839.
[4] T. Arbogast, D. S. Brunson, A computational method for approximating a Darcy-Stokes system governing a vuggy porous medium, Comput. Geosci. 11 (2007) 207-218.
[5] L. Badea, M. Discacciati, A. Quarteroni, Numerical analysis of the Navier-Stokes/Darcy coupling, Numer. Math. 115 (2010) 195-227.
[6] G. S. Beavers, D. D. Joseph, Boundary conditions at a naturally permeable wall, J. Fluid Mech. 30 (1967) 197-207.
[7] W. Chen, M. Gunzburger, D. Sun, Efficient and long-time accurate second-order methods for Stokes-Darcy system, SIAM J. Numer. Anal. 51 (2012) 493-497.
[8] J. Connors, J. Howell, W. Layton, Partitioned timestepping for a parabolic two domain problem, SIAM J. Numer. Anal. 47 (2009) 3526-3549.
[9] M. Discacciati, E. Miglio, A. Quarteroni, Mathematical and numerical models for coupling surface and groundwater flows, Appl. Numer. Math. 43 (2002) 57-74.
[10] D. Erkmen, A. E. Labovsky, Defect-deferred correction method for the two-domain convection-dominated convection-diffusion problem, J. Math. Anal. Appl. 450 (2017) 180-196.
[11] J. Fang, P. Huang, Y. Qin, A two-level finite element method for the steady-state Navier-Stokes/Darcy model, J. Korean Math. Society 57 (2020) 915-933.
[12] F. Hecht, New development in FreeFem++, J. Numer. Math. 20 (2012) 251-265.
[13] W. Jäger, A. Mikelić, On the interface boundary condition of Beavers, Joseph, and Saffman, SIAM J. Numer. Anal. 60 (2000) 1111-1127.
[14] N. Jiang, C. Qiu, An efficient ensemble algorithm for numerical approximation of stochastic Stokes-Darcy equations, Comput. Methods Appl. Mech. Eng. 343 (2019) 249-275.
[15] I. P. Jones, Low reynolds number flow past a porous spherical shell, Proc. Camb. Phil. Soc. 73 (1973) 231-238.
[16] G. Kanschat, B. Riviére, A strongly conservative finite element method for the coupling of Stokes and Darcy flow, J. Comput. Phys. 229 (2010) 5933-5943.
[17] W. Layton, C. Trenchea, Stability of two IMEX methods, CNLF and BDF2-AB2, for uncoupling systems of evolution equations, Appl. Numer. Math. 62 (2012) 112-120.
[18] W. Li, J. Fang, Y. Qin, P. Huang, Rotational pressure-correction method for the Stokes/Darcy model based on the modular grad-div stabilization, Appl. Numer. Math. 160 (2021) 451-465.
[19] K. A. Mardal, X. C. Tai, A robust finite element method for Darcy–Stokes flow, SIAM J. Numer. Anal. 40 (2002) 1605-1631.
[20] M. Mu, J. Xu, A two-grid method of a mixed Stokes-Darcy model for coupling fluid flow with porous media flow, SIAM J. Numer. Anal. 45 (2007) 1801-1813.

[21] Y. Qin, Y. R. Hou, The time filter for the non-stationary coupled Stokes/Darcy model, Appl. Numer. Math. 146 (2019) 260-275.
[22] Y. Qin, Y. R. Hou, P. Z. Huang, Y. S. Wang, Numerical analysis of two grad-div stabilization methods for the time-dependent Stokes/Darcy model, Comput. Math. Appl. 79 (2020) 817-832 .
[23] B. Riviére, Analysis of a discontinuous finite element method for the coupled Stokes and Darcy problems, J. Sci. Comput. 22-23 (2005) 479-500.
[24] P. Saffman, On the boundary condition at the surface of a porous medium. Stud. Appl. Math, 50 (1971) 93-101.
[25] B. Santiago, R. Codina, Unified stabilized finite element formulations for the Stokes and the Darcy problems, SIAM J. Numer. Anal. 47 (2009) 1971-2000.
[26] L. Shan, H. Zheng, W. J. Layton, A decoupling method with different subdomain time steps for the nonstationary Stokes-Darcy model, Numer. Meth. Part. Differ. Equ. 29 (2013) 549-583.
[27] Y. J. Shen, D. F. Han, X. P. Shao, Modified two-grid method for solving coupled Navier-Stokes/Darcy model based on Newton iteration, Appl. Math. J. Chinese Univ. 30 (2015) 127-140.